Supplementary Information

Long-range emissive mega-Stokes inorganic-organic hybrid material with peripheral carboxyl functionality for As (V) recognition and its application in bioimaging

M. Venkateswarulu,[a]Diksha Gambhir,[a] Harpree tKaur,[a] P. VineethDaniel,[a] Prosenjit Mondal,[a]

and Rik Rani Koner[b*]

[a]*School ofBasic Sciences, Indian Institute of Technology Mandi, Mandi-175001, H.P, India.*

[b]*School of Engineering, Indian Institute of Technology Mandi, Mandi-175001, H.P, India.*

12	Fluorescence spectra of PTCA-Cu^{2+} upon the gradual addition of $As^{5+}$and at different slit widths	Figure S14
13	Fluorescence spectra of PTCA-$Cu^{2+}$and H_4PTCAupon the addition of As^{5+}(excitationat 441 and 472 nm)	Figure S15
14	HRMS spectra of PTCA-Cu^{2+} upon titrated with Na_2HAsO_4	Figure S16
15	Benesi-Hildebrand method for the calculation of binding constant for H_4PTCAupon gradual addition of Cu^{2+} ion solution	Figure S17
16	Benesi-Hildebrand method for the calculation of binding constant for PTCA+Cu^{2+}upon gradual addition of As^{5+}ion solution.	Figure S18
17	Fluorescence response of PTCA-Cu^{2+}in presence of As^{5+}at different pH values	Figure S19
18	Plot of fluorescence intensity of PTCA-Cu^{2+} against the concentration of As^{5+}	Figure S20
19	Fluorescence spectra of PTCA-Cu^{2+} (10µM) in DMSO: River water upon the addition of increasing quantities of As^{5+}	Figure S21
20	Fluorescence spectra of PTCA-Cu^{2+} (10µM) in DMSO: Tap water with gradual addition of As^{5+}	Figure S22
21	Ground-state optimized structure of H_4PTCA.	Figure S23
22	Frontier molecular orbitals of H_4PTCA	Figure S24
23	Frontier molecular orbitals of PTCA –Cu^{2+}	Figure S25
24	Optimized structure of the PTCA –As^{5+} complex.	Figure S26
25	Frontier molecular orbital's of PTCA –As^{5+}	Figure S27
26	Time dependent-Density Functional Theory (TD-DFT) derived absorption spectra of H_4PTCA	Figure S28
27	TD-DFT derived absorption spectra of PTCA -Cu^{2+}	Figure S29
28	TD-DFT derived absorption spectra of PTCA –As^{5+}	Figure S30
29	Effect of PTCA-Cu^{2+}concentration on HepG2 cells viability.	Figure S31

Table S1: Comparison of potential of PTCA-Cu^{2+}complextowards As^{5+} ion detection with other reported As^{5+} ion -specific/selective molecular probes.

Sensitive dye	**Excitation/ Emission range**	**Solvent system**	**Reference**
APSAL	λ_{ex} = 350nm λ_{em}= 498 nm	HEPES buffer (Methanol: water)	S. Lohar, A. Sahana, A. Banerjee, A. Banik, S. K. Mukhopadhyay, J. Sanmartín Matalobos and D. Das, *Anal. Chem.*, 2013, **85**, 1778–1783.
Arsenofluorl	λ_{ex} = 385nm λ_{em}= 496 nm	THF	V. C. Ezeh and T. C. Harrop, *Inorg. Chem.*, 2012, **51**, 1213–1215.
DFPPIC	λ_{ex} = 400nm λ_{em}= 530 nm	HEPES buffer	S. Nandi, A. Sahana, B. Sarkar, S. K. Mukhopadhyay and D. Das, *J. Fluoresc.*, 2015, **25**, 1191–1201.
APC	λ_{ex} = 440nm λ_{em} = 532nm	HEPES buffer	A. Banerjee, A. Sahana, S. Lohar, S. Panja, S. K. Mukhopadhyay and D. Das, *RSC Adv.*, 2013, **4**, 3887–3892.
Cu(II)complex $[Cu(n\text{-}BuM)(DEA)]_n$	λ_{ex} = 250nm λ_{em} = 380nm	Aq solution	B. Dey, P. Mukherjee, R. K. Mondal, A. P. Chattopadhyay, I. Hauli, S. K. Mukhopadhyay and M. Fleck, *Chem. Commun.*, 2014, **50**, 15263–15266.
Schiff base	λ_{ex} = 438 nm λ_{em} = 532 nm	DMSO/H_2O (1:9)	S. Lohar, S. Pal, B. Sen, M. Mukherjee, S. Banerjee, and P. Chattopadhyay, *Anal. Chem*. 2014, **86**, 11357−11361.
New Cu(II)complex (PTCA-Cu^{2+})	λ_{ex} = 497 nm λ_{em} = 600 nm	HEPES buffer	Present Work

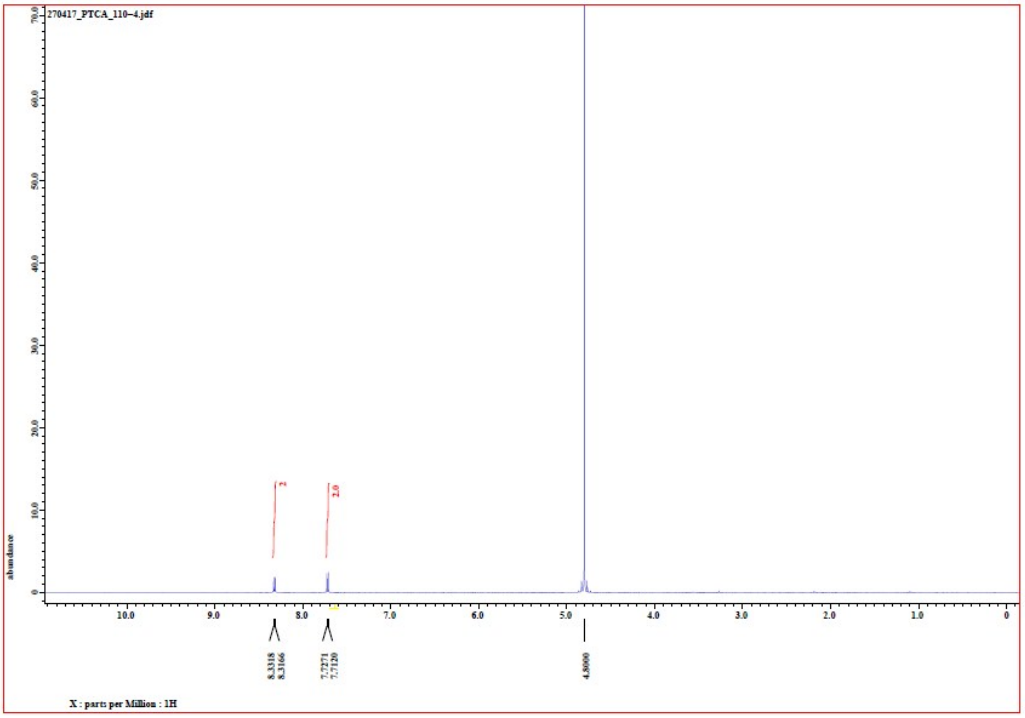

Figure S1.[1]H NMR spectra of **H_4PTCA** in D_2O.

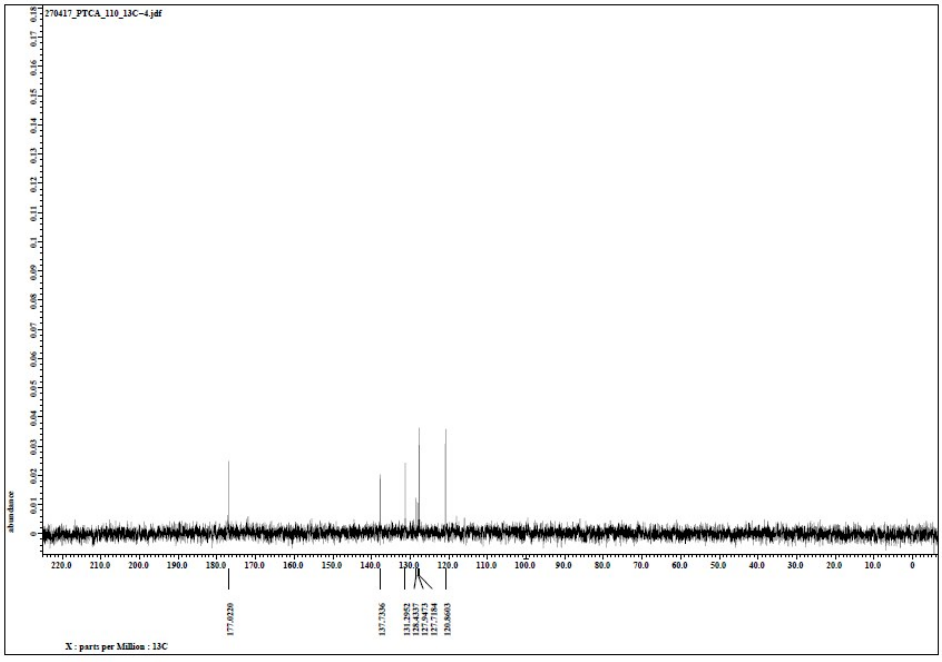

Figure S2.[13]C NMR spectra of **H_4PTCA** in D_2O.

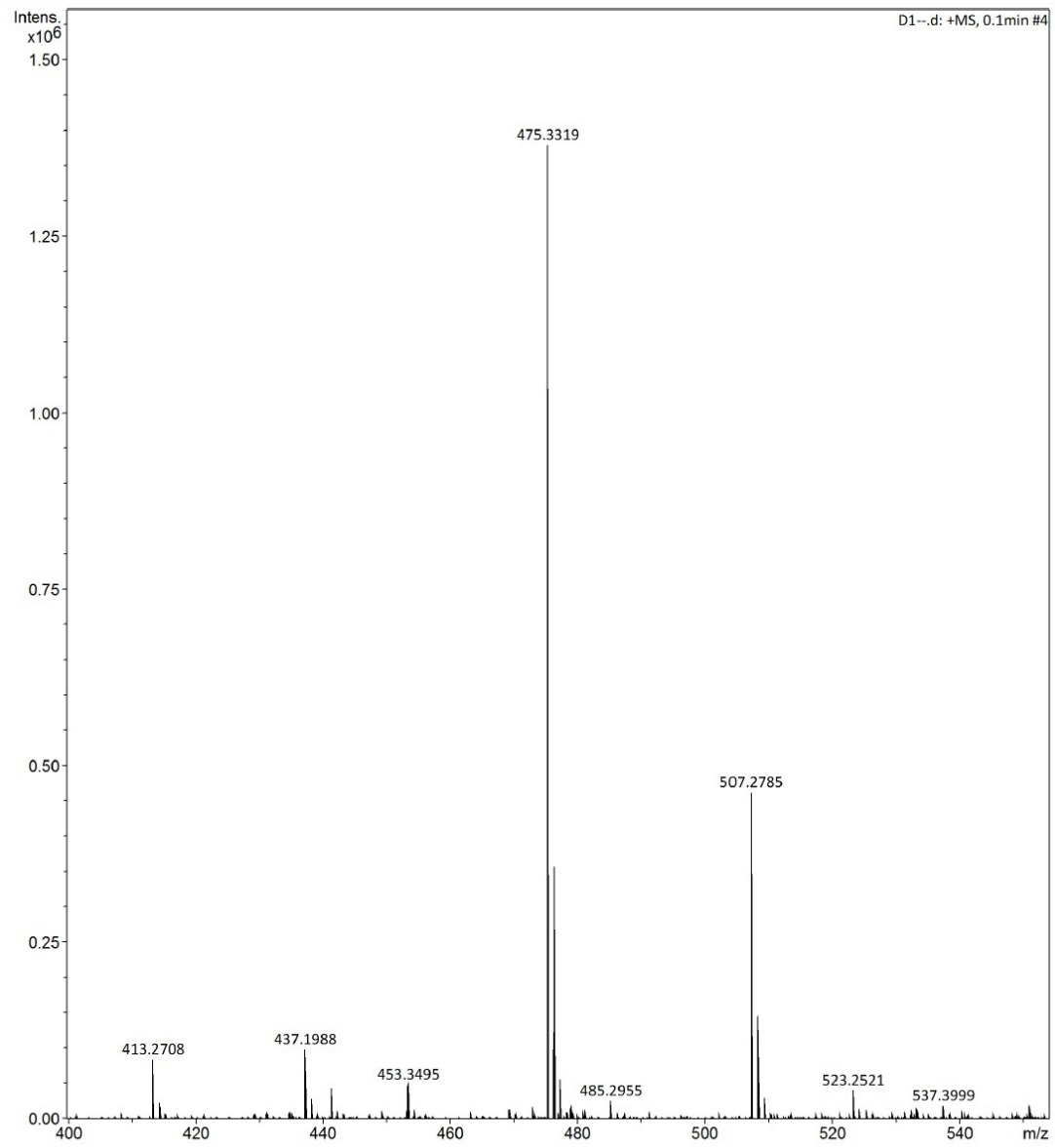

Figure S3.HRMS spectra of **H_4PTCA** in CH_3CN.

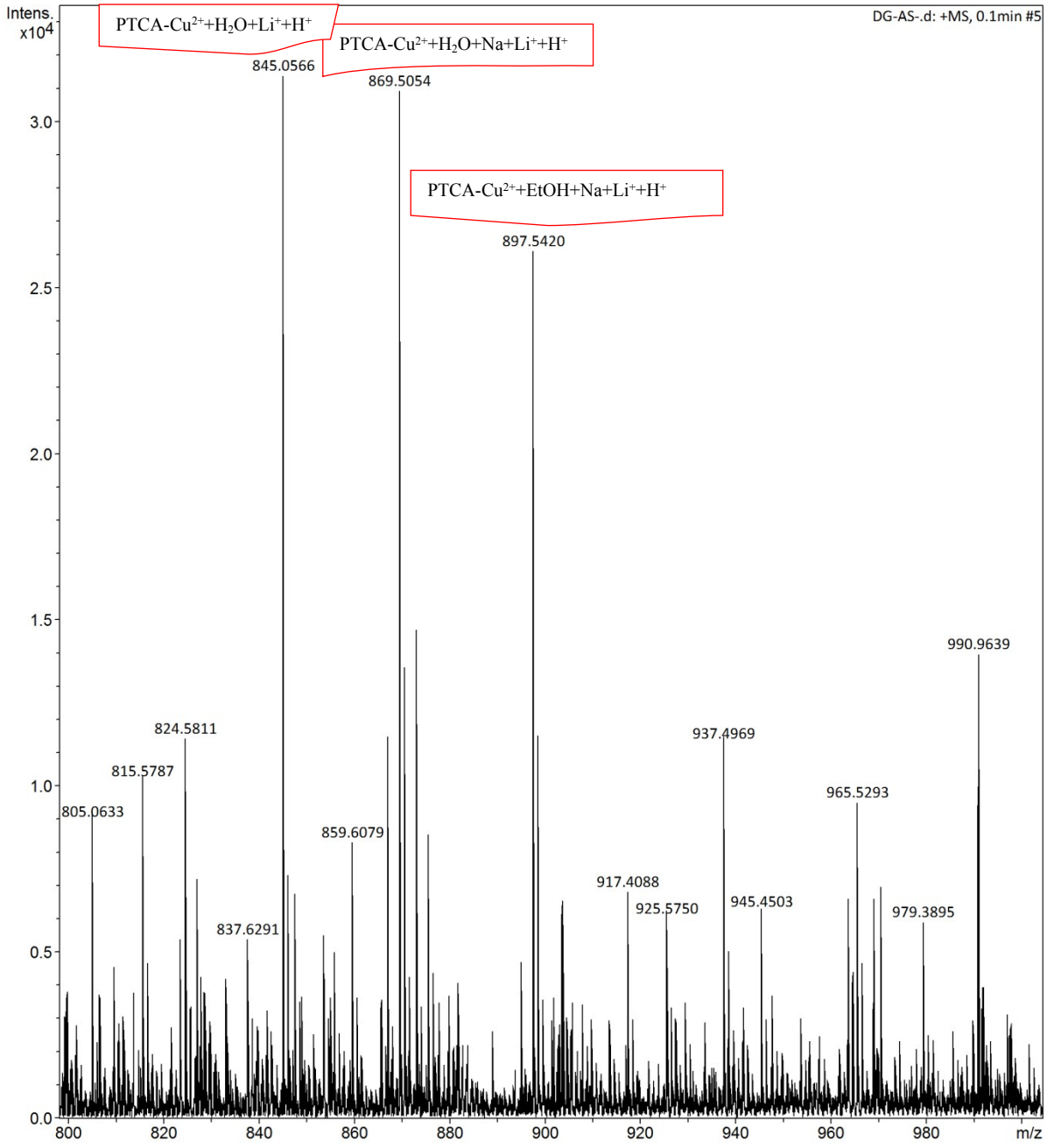

Figure S4.HRMS spectra of **PTCA-Cu^{2+}** in CH_3CN.

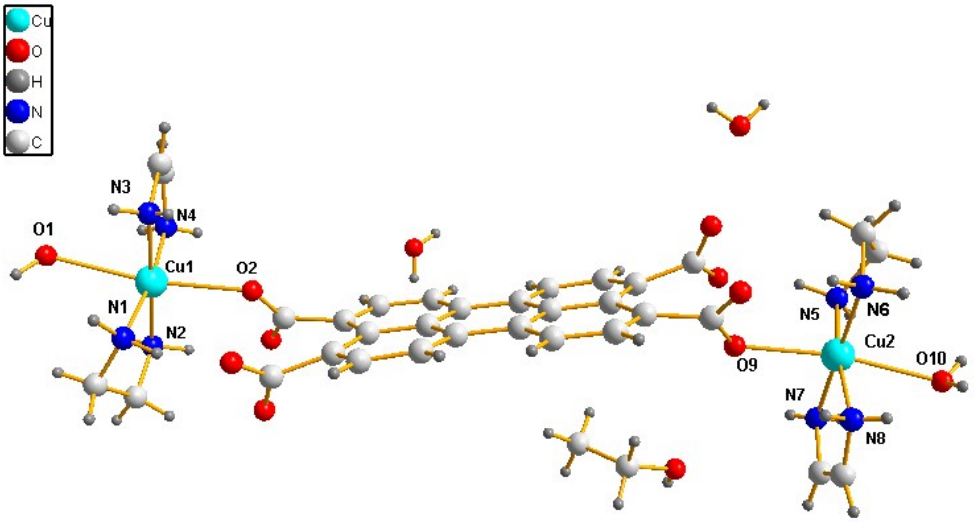

FigureS5. Ball and stick view of **PTCA-Cu^{2+}** complex.

Table S2. Crystal data and Structure Refinement for **PTCA - Cu^{2+}.**

1	Identification code	**PTCA-Cu^{2+}**
2	Empirical formula	$C_{16}H_{27}CuN_5O_9$
3	Formula weight	496.97
4	Temperature/K	293(2)
5	Crystal system, Space group	Monoclinic,$P2_1/c$
6	Unit cell dimension	a =8.579Å, b= 11.285Å, c = 22.518Å α = 90.14, β = 97.84, γ = 89.93
7	Volume/Å^3	2159.6
8	Z, Calculated density	4
9	F(000)	1036.0
10	Crystal size/mm^3	0.1341 X 0.1213 X 0.0717
11	Two Theta range for data	8.78 to 133.74

	collection	
12	Limiting indices(Index ranges)	$-8\leq h\leq 10$, $-13\leq k\leq 9$, $-23\leq 1\leq 26$
13	Reflections collected / unique	7113
14	Data/restraints/parameters	3718/4/299
15	Goodness of fit on F^2	1.030
16	Final R indexes [I>=2σ (I)]	R_1=0.0432,wR_2= 0.1096
17	R indexes [all data]	R_1=0.0452, wR_2= 0.1116
18	Largest diff. peak/hole / eÅ^{-3}	1.04/-0.63

Table S3. Selected Bond Lengths (Å) and angles (deg) of PTCA-Cu^{2+} complex.

Bonds	**Distance/Angle**
O1-Cu1	2.552
O2-Cu1	2.415
N1-Cu1	2.01
N2-Cu1	1.99
N3-Cu1	2.02
N4-Cu1	2.00
O1-Cu1-O2	170.79
N1-Cu1-N2	84.62
N3-Cu1-N4	84.91
N1-Cu1-N3	95.11
N2-Cu1-N4	95.17

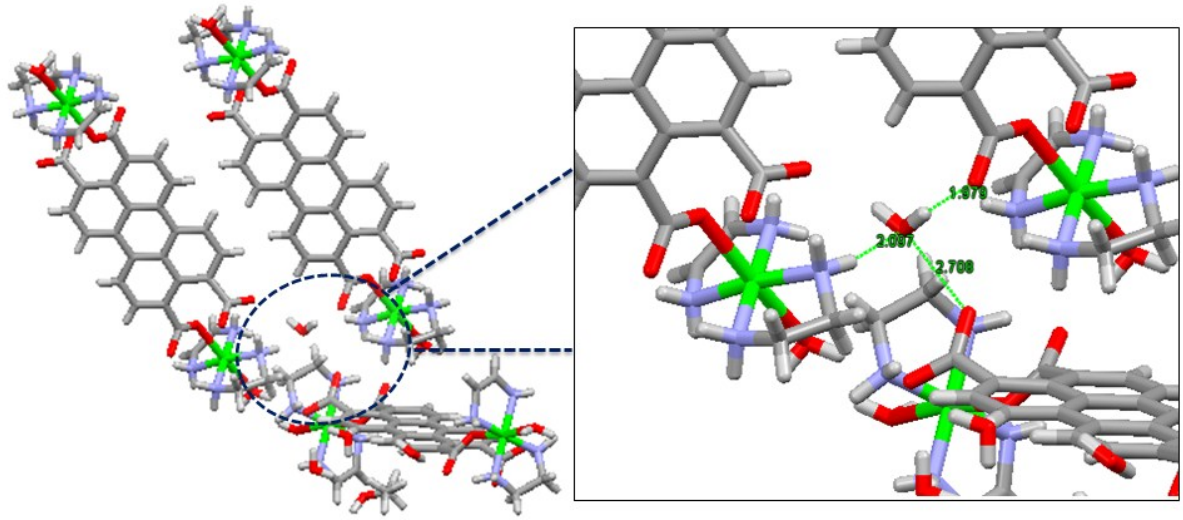

Figure S6. Hydrogen bond between the uncoordinated carboxylate oxygen , aqua molecule and NH of the ethylene diamine unit.

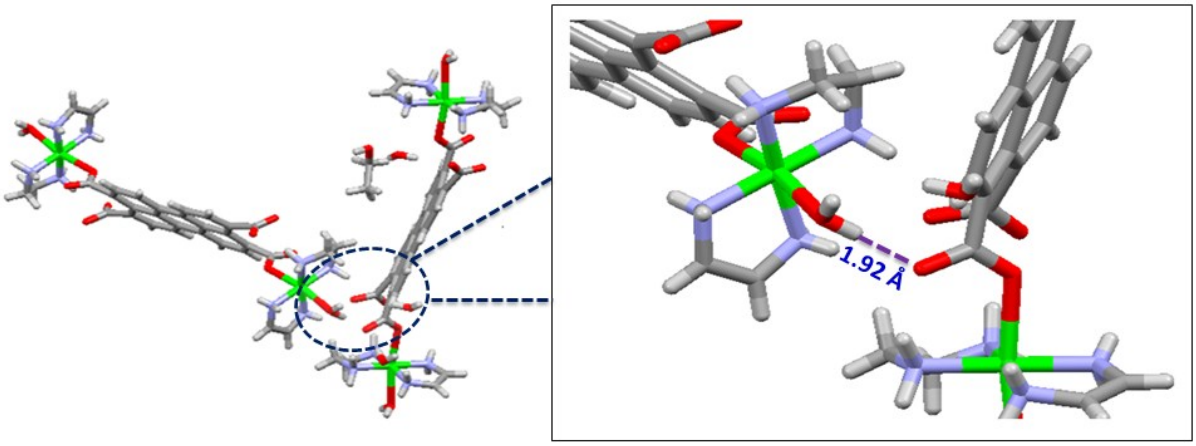

Figure S7. The carboxylate unit forms hydrogen bond with coordinated aqua molecule (Cu─H_2O••••OOC-Cu).

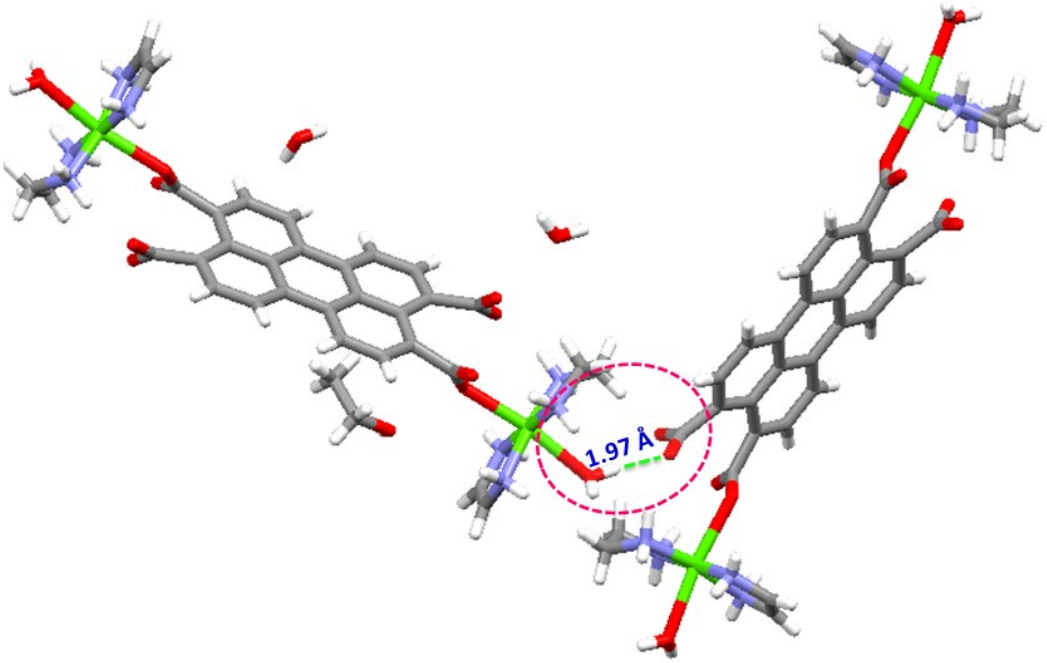

Figure S8. The free carboxylate unit forms hydrogen bonds with coordinated aqua molecule (Cu─H_2O••••OOC-) of neighbouring unit.

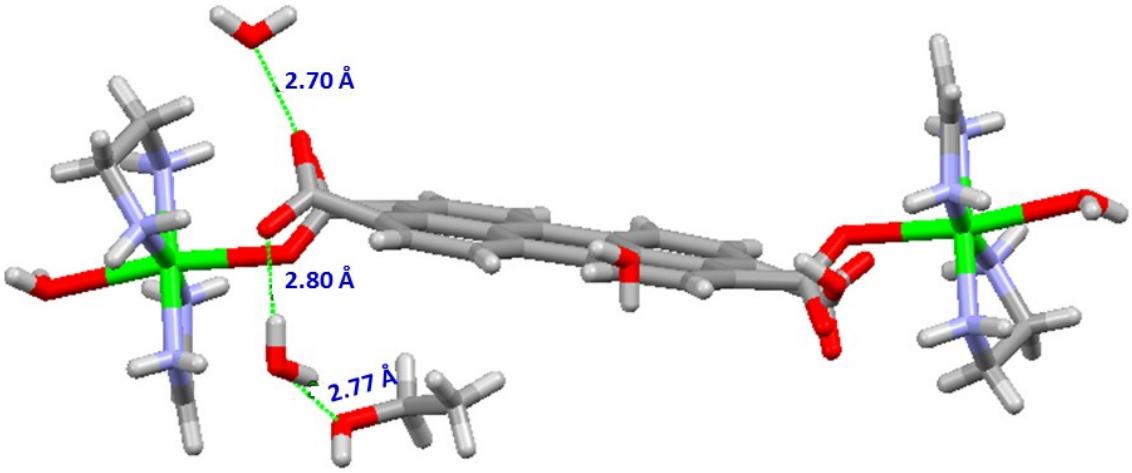

Figure S9. Hydrogen bonds between the uncoordinated carboxylate and solvent molecules.

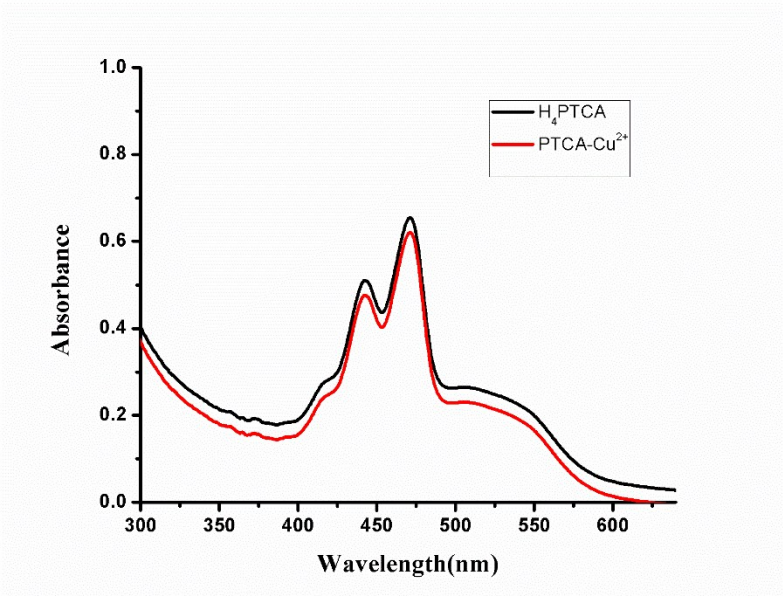

Figure S10: UV-vis spectra of**H_4PTCA** and**PTCA-Cu^{2+}** (10µM) in DI H_2O buffered with HEPES (1mM), pH = 7.2.

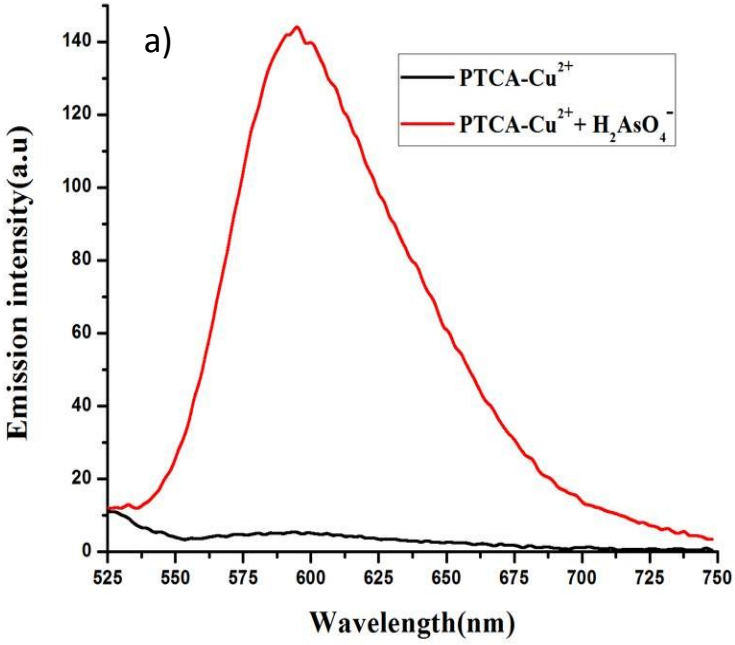

Figure S11. Fluorescence spectra of **PTCA-Cu^{2+}** (10µM) inDI H_2O buffered withHEPES (1 mM), pH = 7.2 upon the addition of As^{5+} (166 µM) (excitation at 497 nm and emission at 600 nm and slit width 5/10)

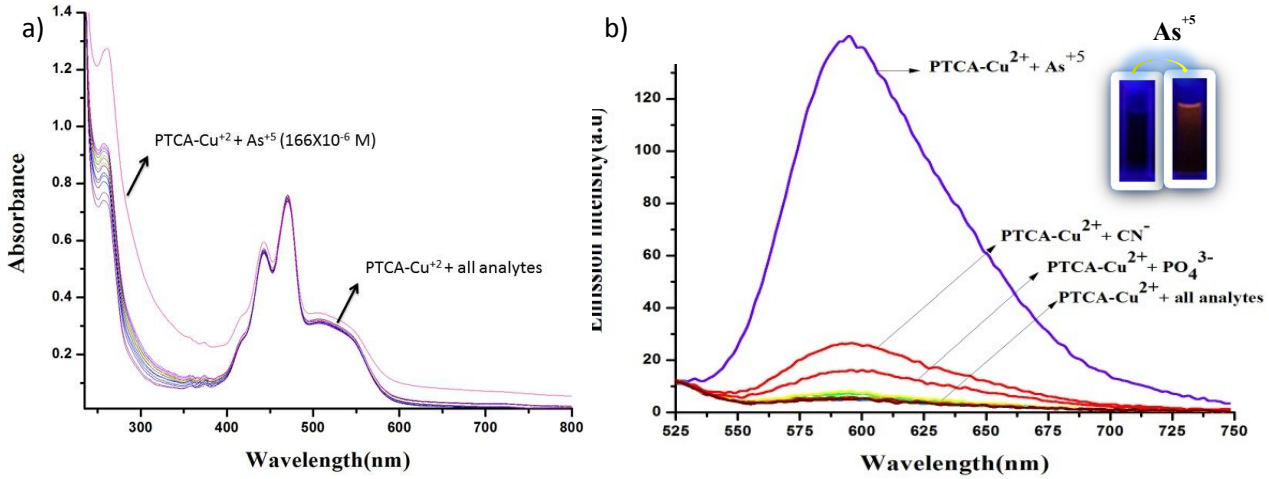

Figure S12a). UV-vis spectra and **b)** Fluorescence spectra of **PTCA-Cu^{2+}** (10µM) inDI H_2O buffered withHEPES (1 mM), pH = 7.2 upon the addition of 166 µM different anions (Cl^-, F^-, Br^-, HSO_4^-, CN^-, NO_3^-, PO_4^{3-}, ClO_4^- and CH_3COO^-) and cations(As^{3+}, As^{5+}, Li^+, Na^+, K^+, Ca^{2+}, Mg^{2+}, Fe^{2+}, Fe^{3+}, Mn^{2+}, Co^{2+}, Ni^{2+}, Cd^{2+}, Hg^{2+}, Zn^{2+}, Sn^{2+}, Sr^{2+}, Al^{3+}, Cr^{3+}, Bi^{2+}, Sb^{2+}).

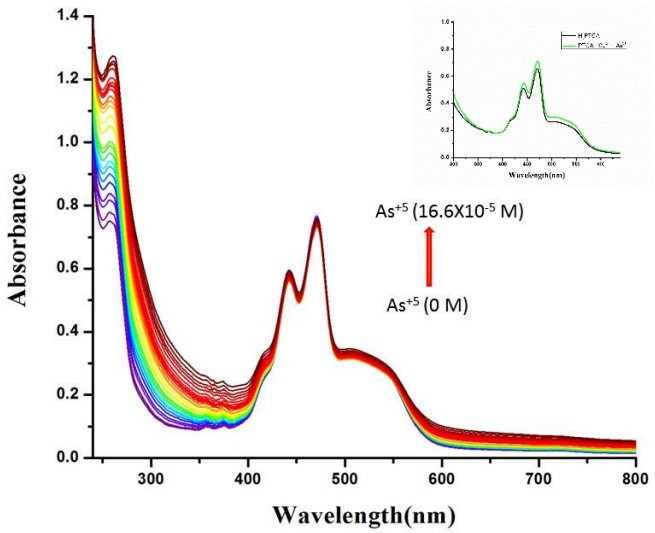

Figure S13. UV-vis spectra of **PTCA-Cu^{2+}** (10µM) in DI H_2O buffered withHEPES (1 mM), pH = 7.2 upon the addition of increasing quantities of As^{5+} (0 to 166 µM) (**inset**: UV-vis spectra of H_4PTCA and upon addition of As^{5+}).

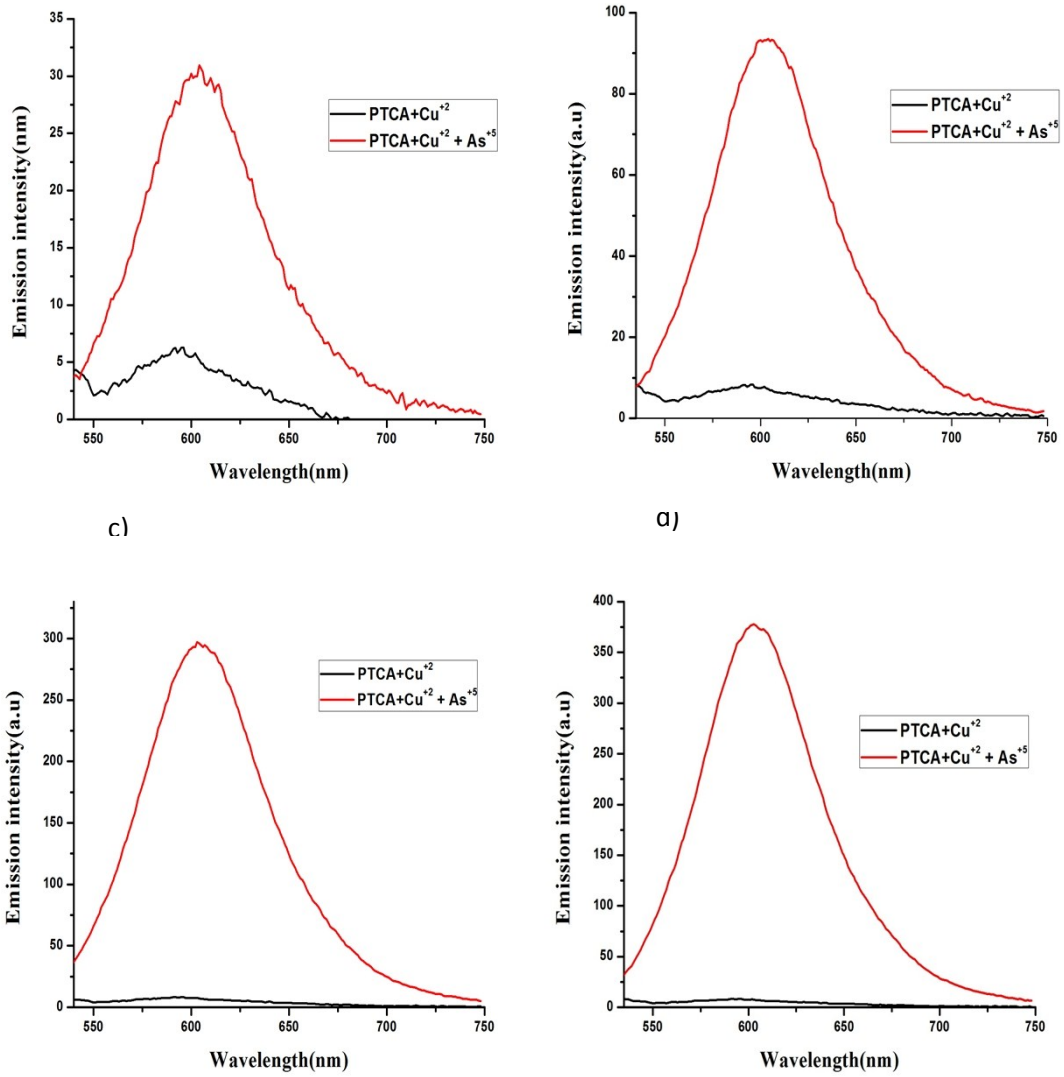

Figure S14a-d. Fluorescence spectra of **PTCA-Cu^{2+}** (10μM) inDI H_2O buffered withHEPES (1 mM), pH = 7.2 upon the addition of As^{5+} (166 μM) (excitation at 497 nm and emission at 600 nm and slit width 5/5, 10/5, 5/20 and 10/10 respectively.

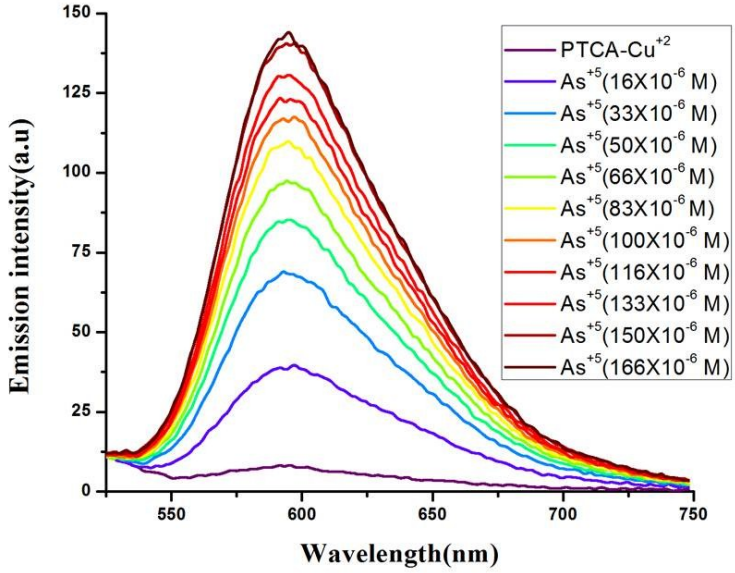

Figure S14e. Fluorescence spectra of **PTCA-Cu^{2+}** (10μM) in DI H_2O buffered withHEPES (1 mM), pH = 7.2 upon the addition of increasing quantities of As^{5+} (0 to 166 μM)(excitation at 497 nm and emission at 600 nm and slit width 5/10).

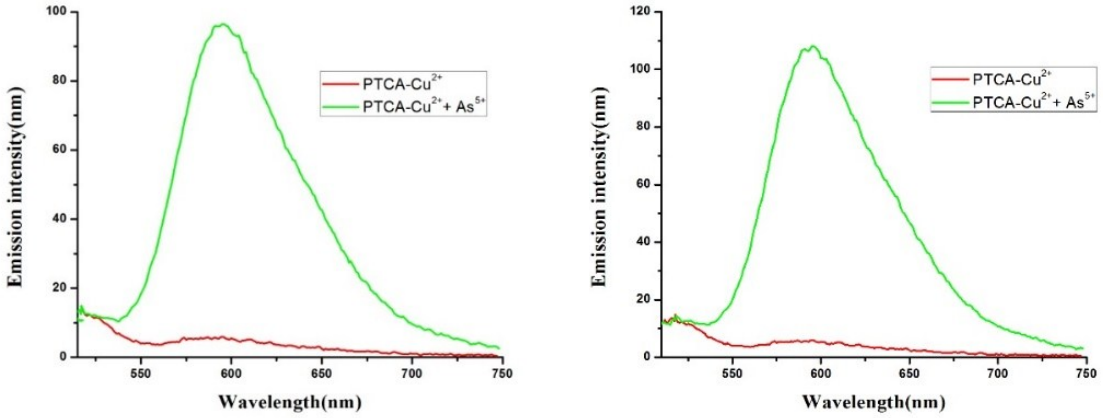

Figure S15a. Fluorescence spectra of **PTCA-Cu^{2+}**(10μM) in DI H_2O buffered with HEPES (1mM), pH = 7.2 upon the addition of As^{5+}ion (0 to 166 μM) (excitation at 441 nm and 472 nm respectively and emission at 600 nm)

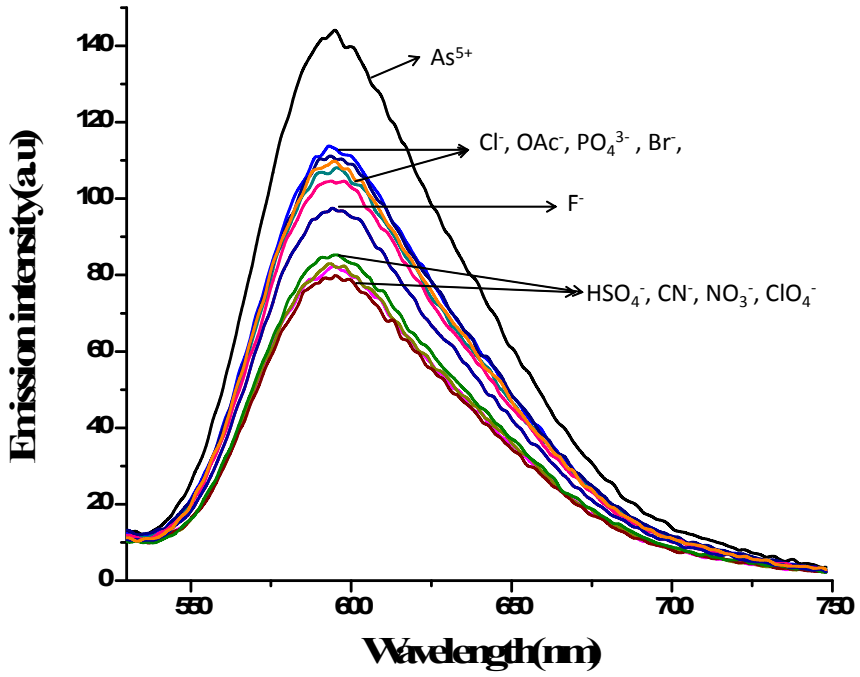

Figure S15b. Emission spectra of **H_4PTCA** (10 μM) in H_2O buffered withHEPES (1 mM), pH = 7.2 upon the addition of 166 μM different anions (Cl^-, F^-, Br^-, HSO_4^-, CN^-, NO_3^-, PO_4^{3-}, ClO_4^- and CH_3COO^-) excitation at 497 nm and emission at 600 nm.

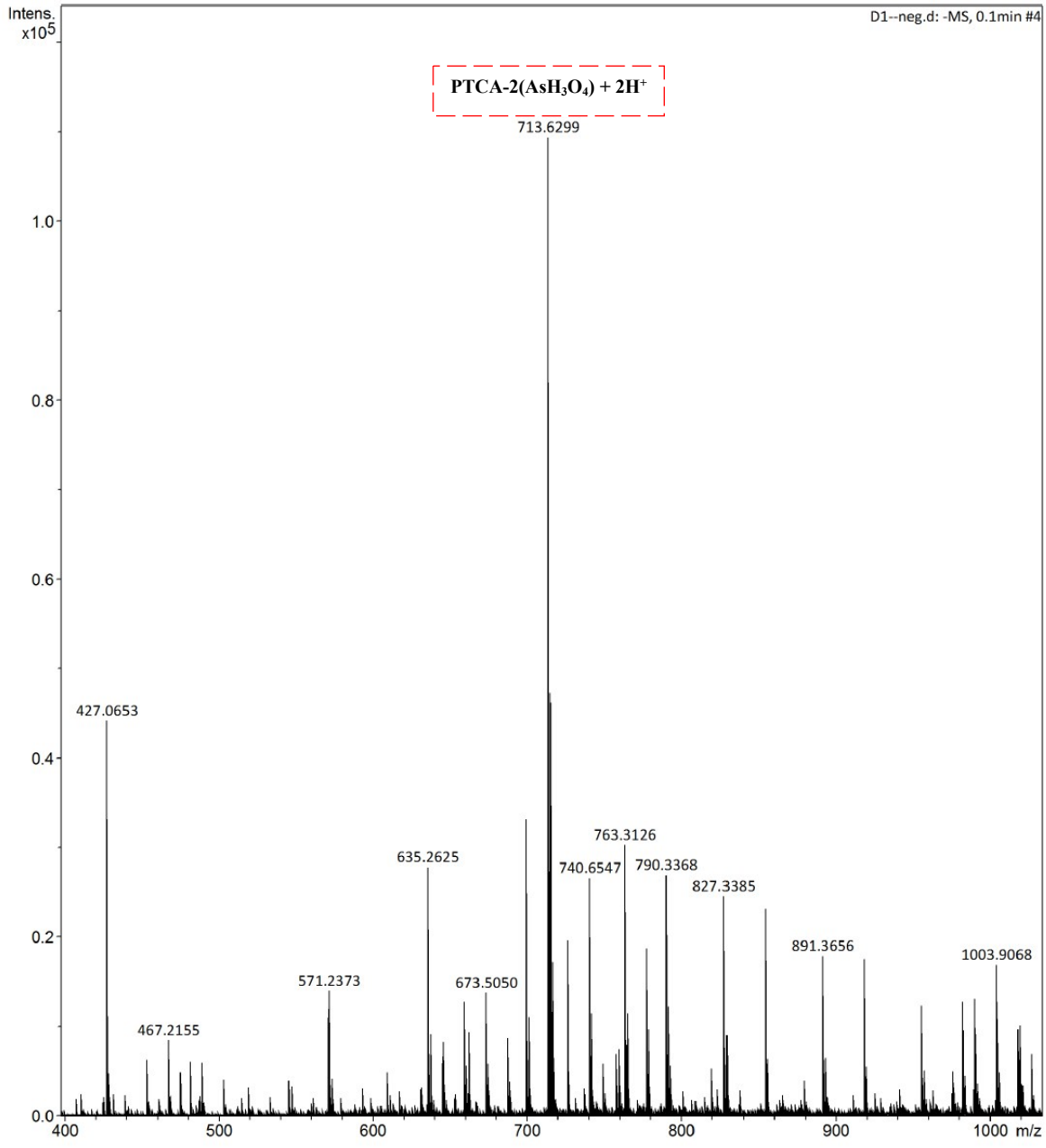

Figure S16a.HRMS spectra of **PTCA-Cu^{+2}** upon titrated with Na_2HAsO_4in acetonitrile.

(PTCA-2(AsH_3O_4)+2H^+)-$C_{24}H_{20}As_2O_{16}^{+2}$713.9183.

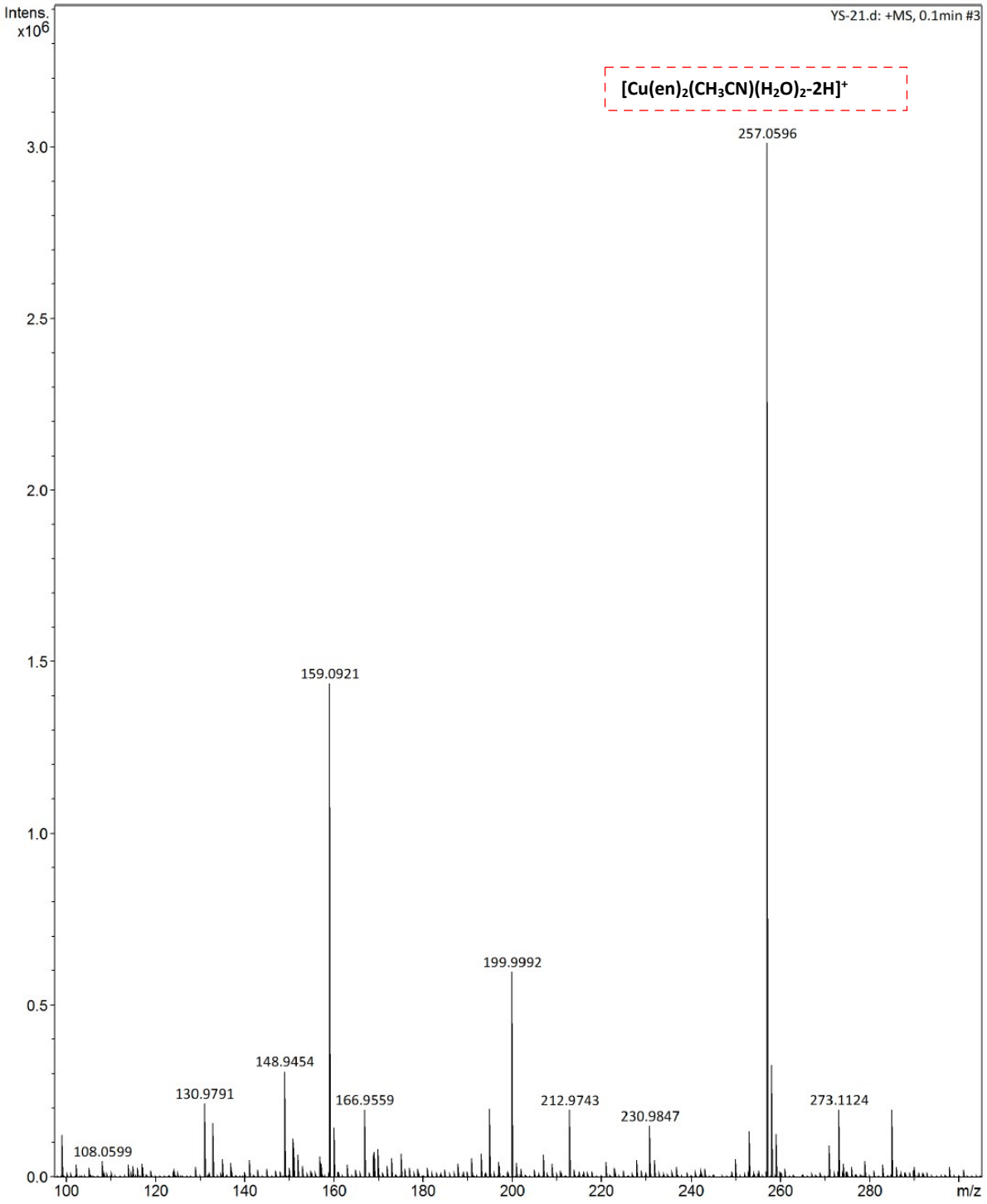

Figure S16b.HRMS spectra of **PTCA-Cu^{+2}** upon titrated with Na_2HAsO_4 in CH_3CN.

Binding constant calculation

Methods for association or stability constant calculation: Binding properties of **PTCA-Cu^{2+}**towards with As^{5+} complexes were determined by fluorescence titrations. All the measurements were performed by titrating **PTCA-Cu^{2+}** with As^{5+} ion in H_2O (HEPES buffered, pH ~7.2) at 25°C. Initial concentrations of the **PTCA-Cu^{2+}** and As^{5+} were 10 µM and 1mM, respectively. Each titration was performed by several measurements with varying metal ion concentrations in order to avoid dilution error, and the association constants were calculated using Benesi-Hildebrand method.

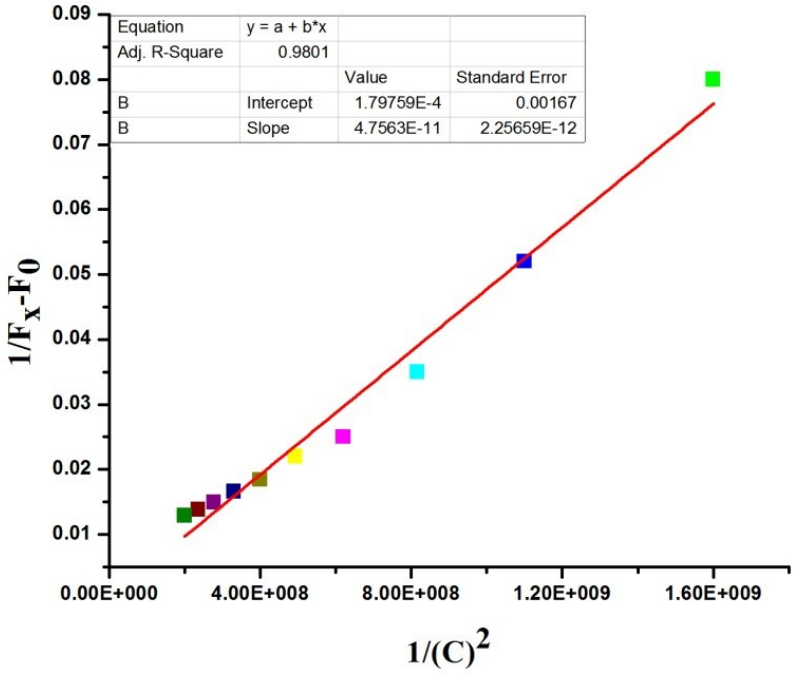

Figure S17. Benesi-Hildebrand method for the calculation of binding constant for H_4PTCAupon gradual addition of Cu^{2+}ion solution (Excitation at 497 nm in H_2O buffered with HEPES (1 mM), pH = 7.2.Solution was incubated for 5 min at 25ºC.

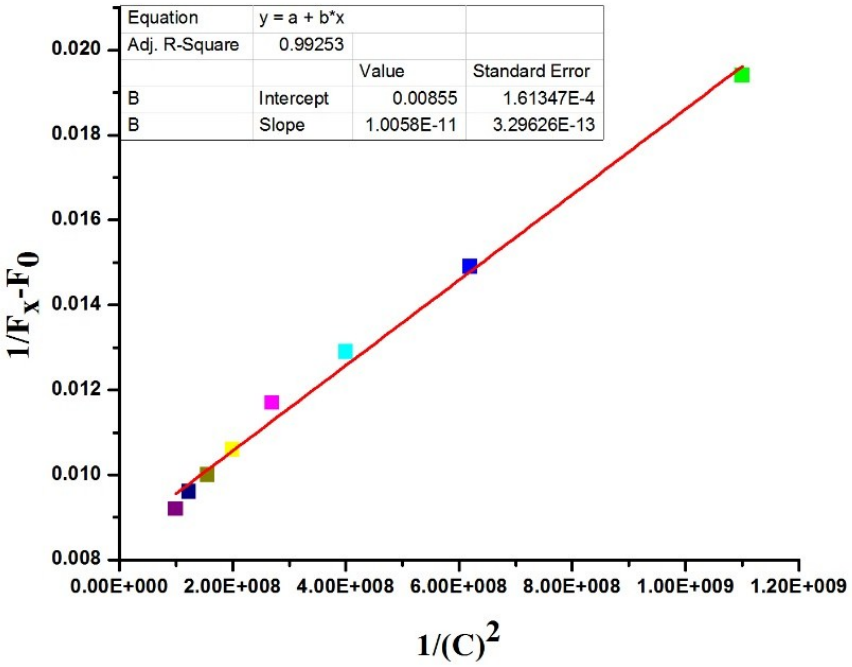

Figure S18. Benesi-Hildebrand method for the calculation of binding constant for PTCA+Cu^{2+}upon gradual addition of As^{+5}ion solution (Excitation at 497 nm in H_2O buffered with HEPES (1 mM), pH = 7.2.Solution was incubated for 5 min at 25ºC.

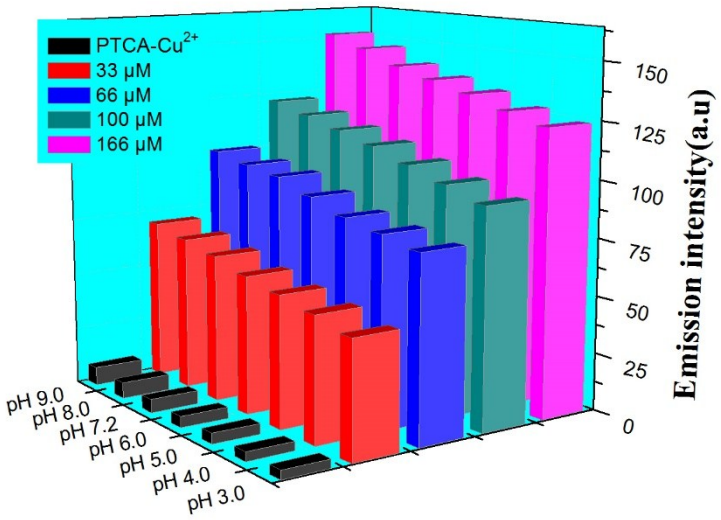

Figure S19. Fluorescence response of **PTCA-Cu^{2+}**(10 μM) in H_2O buffered with HEPES (1 mM) at different pH values (λex = 497 nm) upon addition of different concentrations of Na_2HAsO_4.

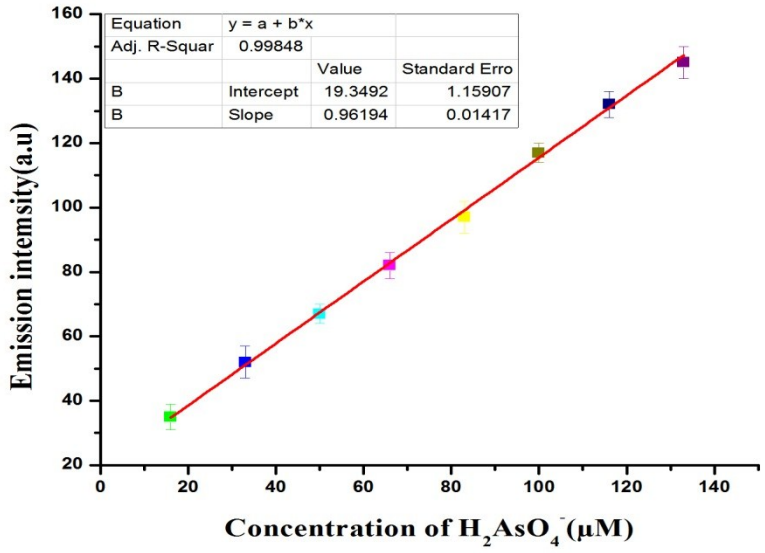

Figure S20. Plot of fluorescence intensity of **PTCA-Cu^{2+}**(10 μM) in DI H_2O buffered with HEPES (1 mM, pH = 7.2), excitation at 497 nm as a function of the concentration of As^{5+}.

Detection of As^{5+} ion in real samples:

River water and tap water were used as real samples for analysis of **As^{5+}** ion. These real samples used as solvents for the preparation of different concentrations of **As^{5+}** ion standard solutions to record the fluorescence spectra. The detection procedure for river water and tap water is the same as that used above. We are in the process of collecting various real-world samples which contain **As^{5+}** ion and would like to apply our probe in future to detect the presence of those metal ions.

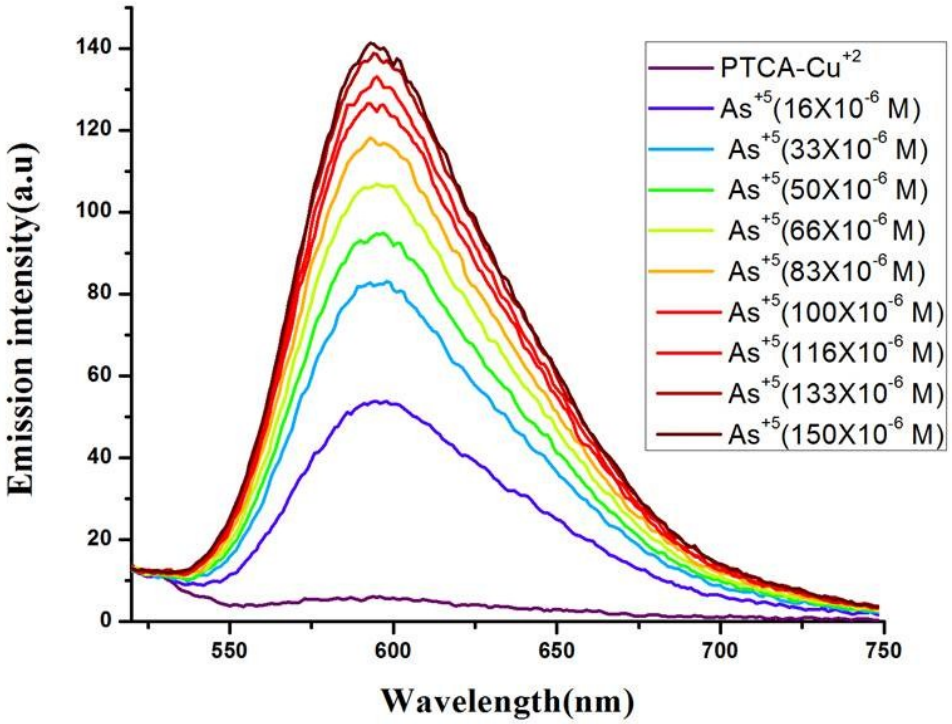

Figure S21. Fluorescence spectra of PTCA-Cu^{2+} (10μM) in DMSO: River water (, v/v) upon the addition of increasing quantities of As^{5+} (0 to 150μM)(excitation at 497 nm and emission at 600 nm).Solution was incubated for 5 min at 25ºC.

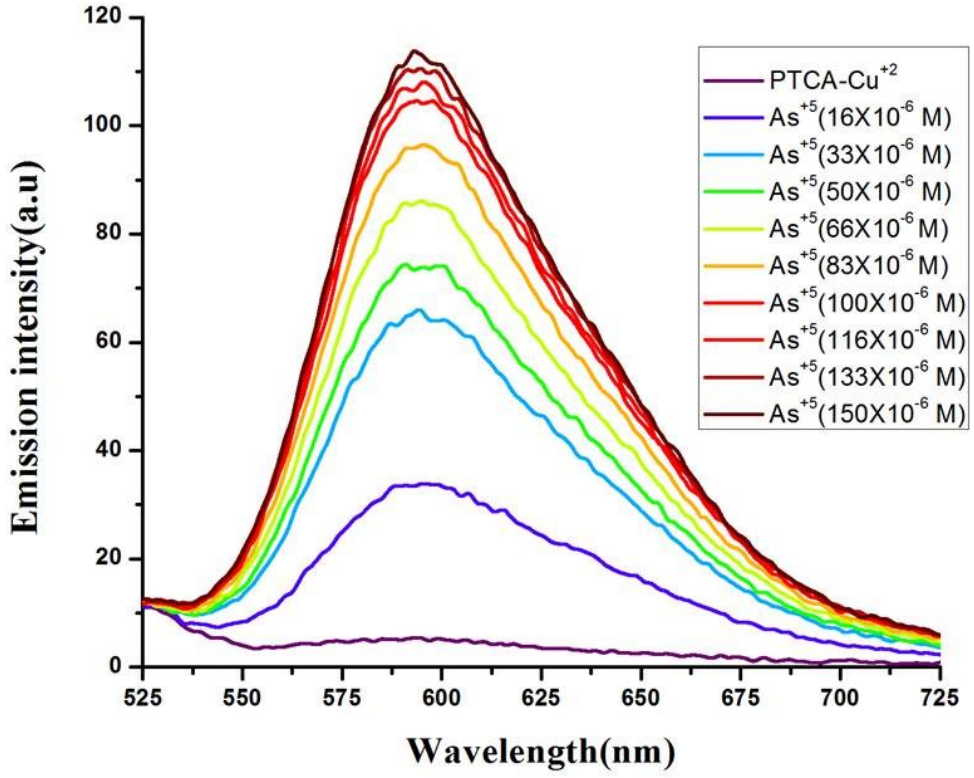

Figure S22. Fluorescence spectra of PTCA-Cu^{2+} (10μM) in DMSO: Tap water (, v/v) upon the addition of increasing quantities of As^{5+} (0 to 150 μM)(excitation at 497 nm and emission at 600 nm).Solution was incubated for 5 min at 25ºC.

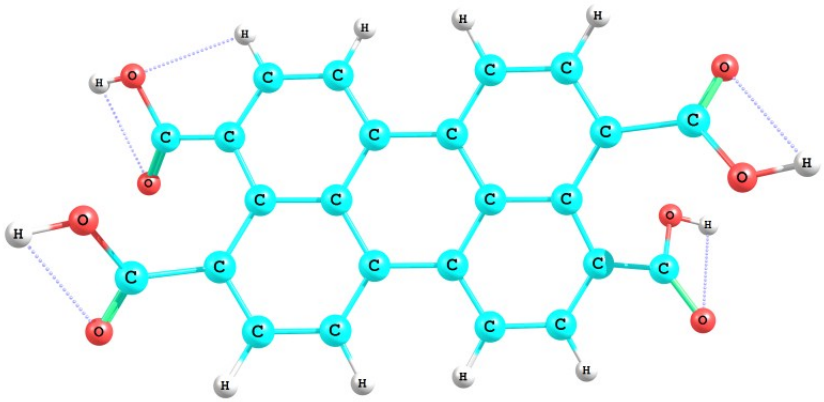

Figure S23. Ground-state optimized structure of **H_4PTCA.**

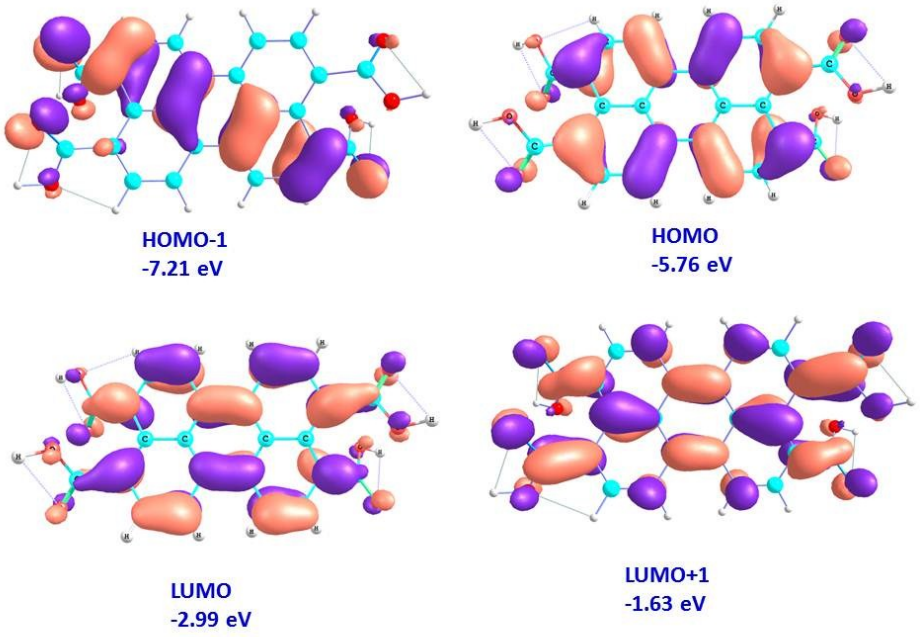

Figure S24. Frontier molecular orbital's of **H_4PTCA** (isocontour at 0.03 au)**.**

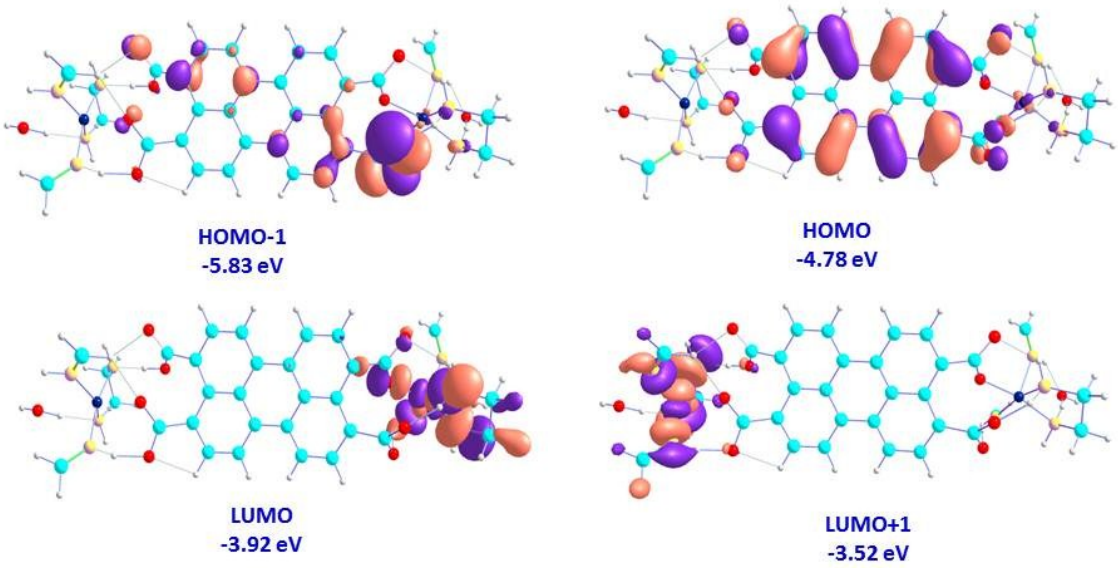

Figure S25. Frontier molecular orbitals of **PTCA-Cu^{2+}** complex (isocontour at 0.03 au).

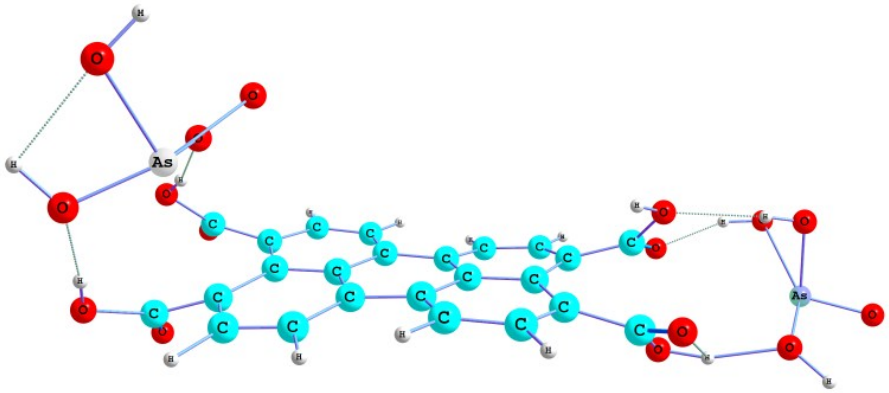

FigureS26. Optimized structure of the **PTCA –As^{5+}**complex.

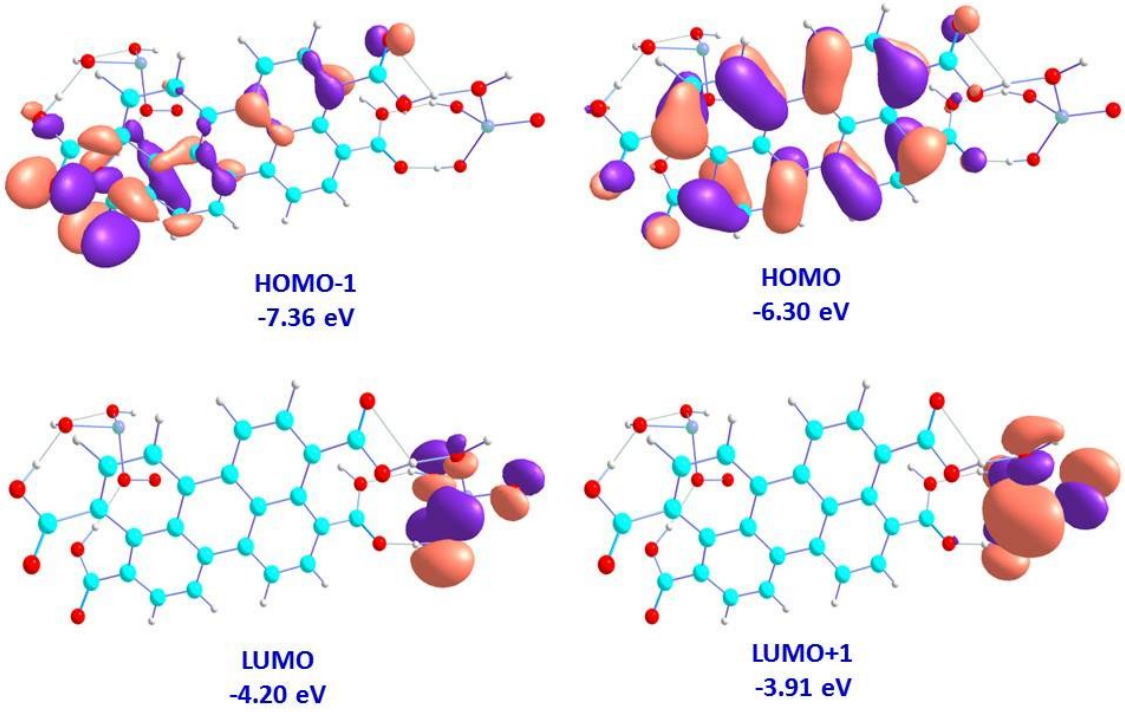

FigureS27. Frontier molecular orbitals of **PTCA –As^{5+}**complex (isocontour at 0.03 au).

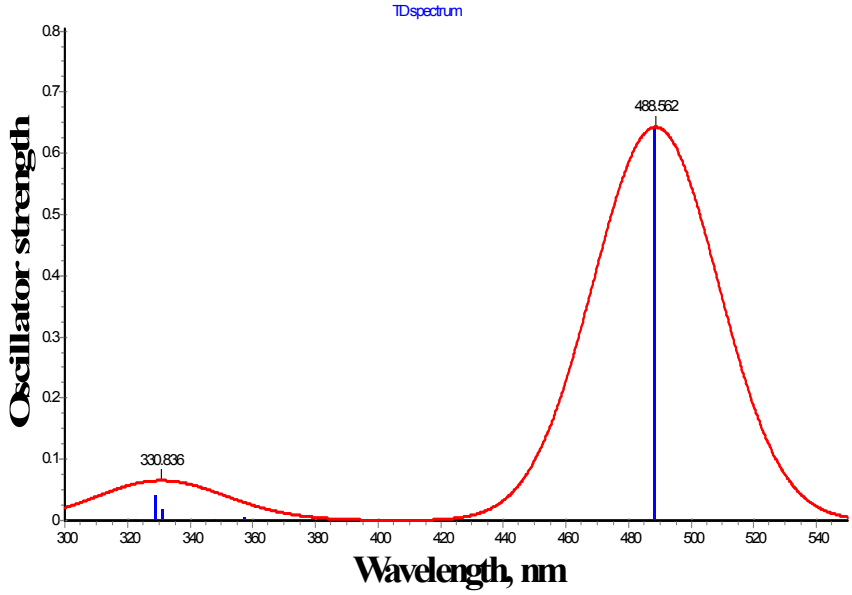

Figure S28. TD-DFT derived absorption spectra of the **H_4PTCA**.

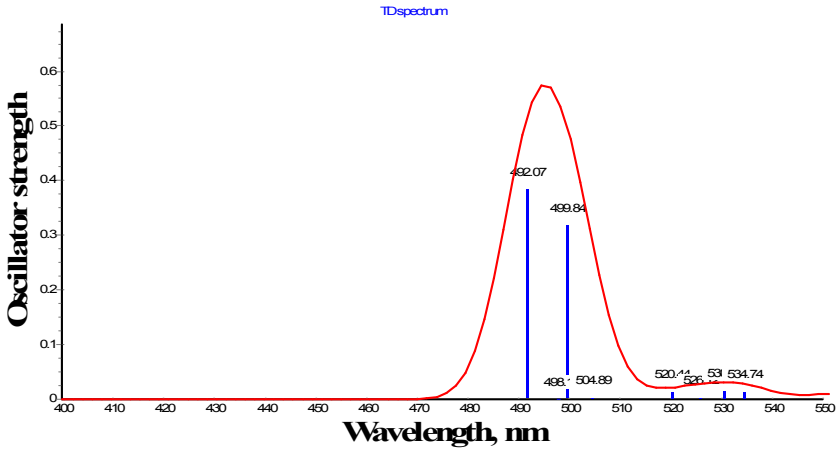

Figure S29. TD-DFT derived absorption spectra of PTCA-Cu^{2+} complex (isocontour at 0.03 au).

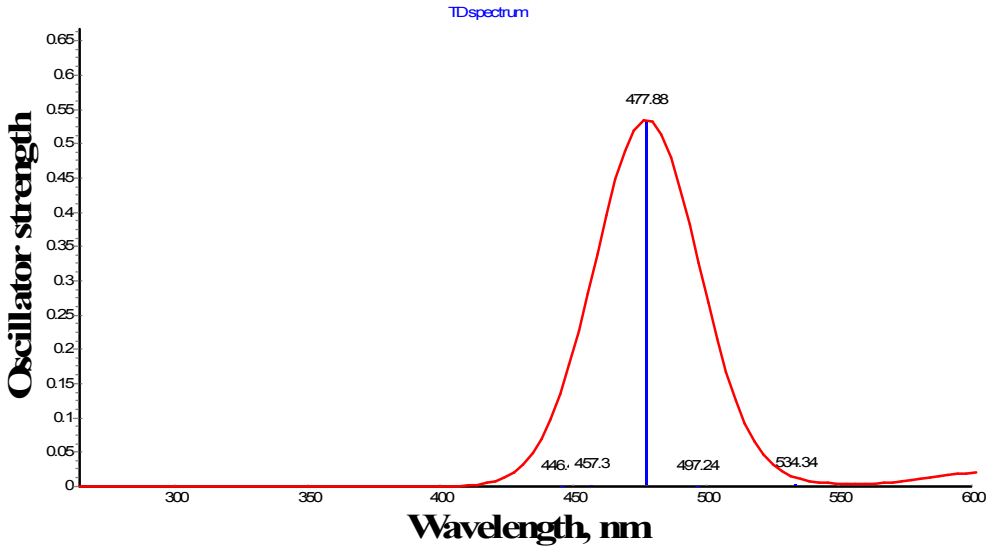

Figure S30. TD-DFT derived absorption spectra of PTCA-As^{5+} complex (isocontour at 0.03 au).

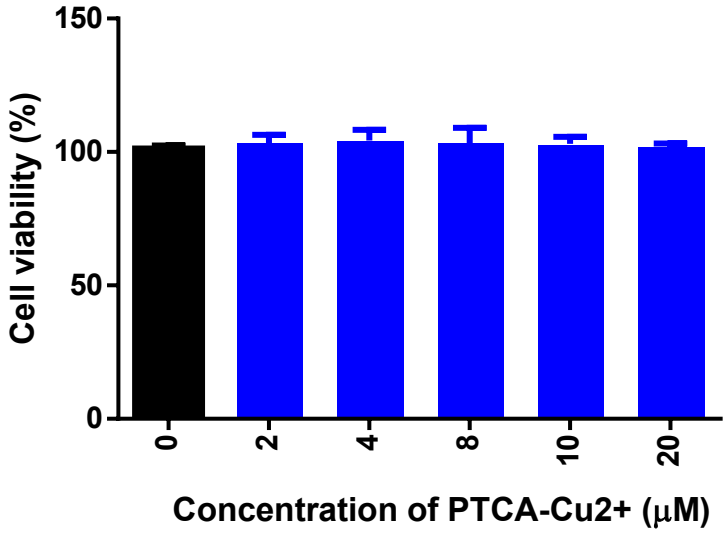

Figure S31. Effect of PTCA-Cu^{2+} on HepG2 cells viability. (a) HepG2 cells were exposed to different doses of PTCA-Cu^{2+} for 24h andMTT assay were performed to determine the viability. Viability was represented as percentage (%) of control. All data wererepresented as Mean ± SE (Standard Error) of two-three independent experiments in triplicate.